Proceedings of the 4th WSEAS International Conference on Fluid Mechanics and Aerodynamics, Elounda, Greece, August 21-23, 2006 (pp266-274)

Optimization Method for Centrifugal Pump Impellers: Coupling of Hybrid Genetic Optimization and Potential Flow solver

Nikolas Antonakis
Laboratory for Aero and Hydrodynamics
Technical University of Delft
Leeghwaterstraat, 21
2628 CA Delft
Netherlands

Ronald Dijkers
Flowserve Corporation
Lansinkesweg 30
7553 AE Hengelo
Netherlands

Remko Westra
Engineering Fluid Dynamics
University of Twente
7500 AE Enschede

Abstract: - The performance of an industrial radial-flow pump impeller is iteratively optimized. Using a potential flow model to compute the flow through the blade channel, an objective function is constructed to take into account the desirable and the actual performance characteristics. The impeller geometry is efficiently parametrized to reproduce sufficient geometrical variations. A hybrid optimization method is used to minimize the objective function. The concept of the hybrid approach is to employ a global stochastic optimization method for the diversification of the search space and a deterministic local method for intensifying the final search towards the optimum. Results present an optimised impeller with improved performance but also a clear trade-off among contradictory objectives.

Key-Words: - Potential flow, Genetic algorithm, Hybrid, Design, Optimization, Centrifugal pump

1 Introduction

The design of centrifugal pump impellers heavily relies on the experience of the engineer to select and evaluate the many possible geometrical variations in the search for the most suitable setup. It is often not clear which is the best strategy to pursue due to complex flow phenomena that occur inside the blade channel and contradictory performance requirements that have to be satisfied. The development of advanced computational codes that compute the flow inside the machine (CFD) has been a breakthrough in the field of turbomachinery design but do not provide the capability of automatically generating an optimised design.

Using optimization methods, the design is optimized iteratively in terms of a cost function specified by the designer. The objective of this work is to present such an optimization method and its application in an industrial centrifugal pump.

The direct optimization requires a flexible parametric description of the geometry (van Os [1]). An objective function has to be defined which involves among many objectives the desirable pumping head, efficiency and cavitation characteristics. Therefore the necessity for multi-objective optimization arises.

Genetic Algorithms (GA) are a promising solution to this complicated optimization problem since they are not affected as much as classical methods by local optima. Hence they are robust in terms of finding a

global optimum but require an augmented number of flow computations. The counterweight to the increased computing requirements will be the use of an efficient potential flow model. The potential flow model has been acknowledged to predict head, cavitation inception and hydraulic power with a sufficient accuracy for pump impellers working at design or near-design conditions (van Esch and Kruyt [2]). Furthermore the numerical approach integrated in the potential flow model used here allows fast, low CPU cost, three-dimensional computations.
The concept of a hybrid optimization is employed; the power of the genetic algorithm to diversify within the search space is combined with a deterministic method (Sherif et al. [3]). The latter local method is used during the final step of the optimization to refine the search in the neighbourhood of GA's proposed solution.
Most optimization attempts are based on single-point optimization, that is optimization at a single set of operating conditions. This may result in an impeller that at the design operating conditions is exceptional, but for other operating conditions has poor performance. In conjunction with high industry requirements the application of multi-point optimization is motivated.

Nomenclature

$\vec{v}$	**absolute velocity**	**[m/s]**
$\vec{w}$	**relative velocity**	**[m/s]**
Ω	**angular velocity of impeller**	**[rad/s]**
ρ	**fluid density**	**[kg/m^3]**
r	**radius**	**[m]**
D	**impeller diameter**	**[m]**
ϕ	**velocity potential**	**[-]**
p	**static pressure**	**[Pa]**
c_D	**dissipation coefficient**	**[-]**
Re	**Reynolds number**	**[-]**
Re_θ	**momentum thickness Re**	**[-]**
H	**Head**	**[m]**
Q	**volume flow rate**	**[m^3/s]**
H	**efficiency**	**[-]**
η_ω	**specific speed** $= \Omega Q^{1/2}/(gH)^{3/4}$	**[-]**
Ψ	**head coeeficient** $= gH/(\Omega R)^2$	**[-]**
Φ	**flow coefficient** $= Q/(\Omega R^3)$	**[-]**
κ	**cavitation coefficient** $= g \cdot NPSH/(\Omega R)^2$	**[-]**

2 Flow model

For most pumps operating near design conditions, the core of the flow is governed by the influence of centrifugal and Coriolis forces and can thus be fairly accurately predicted by means of a potential flow.

2.1 Potential Flow Model

The potential-flow approximation means that the flow is considered irrotational ($\nabla \times \vec{v} = 0$) and solenoidal ($\nabla \bullet \vec{v} = 0$).
The following assumptions can be made to support the choice of the potential-flow model,

- Mach numbers are small enough to justify the assumption of incompressibility ($Ma^2 << 1$).
- Due to high Re numbers all viscous effects are concentrated within boundary layers which are thin compared to the width of the impeller passage (van Esch [4]). No boundary layer separation occurs in design conditions.
- Turbulence intensity Tu,
$$Tu^2 = \frac{v'^2}{v^2} \tag{1}$$
will be in practice 5% or less for the core of the flow, which means that the relative importance of Reynolds stresses is of order 10^{-3} (van Esch [4]).
- The fluid enters the impeller free of vorticity.

The core flow field can then be described by a velocity potential ϕ,
$$\nabla \phi = \vec{v} \tag{2}$$
while the equation of continuity reduces to the Laplace equation,
$$\nabla^2 \phi = 0 \tag{3}$$
The pressure distribution can be computed from the unsteady Bernoulli equation,
$$\left.\frac{\partial \phi}{\partial t}\right|_R + (\vec{w} - \vec{v}) \bullet \nabla \phi + \frac{1}{2} \vec{v} \bullet \vec{v} + \frac{p}{\rho} = c(t) \tag{4}$$

The influence of stationary parts on the rotating impeller is not taken into account (free impeller). The flow can be assumed stationary in the rotating frame of reference, i.e.
$$\left.\frac{\partial \phi}{\partial t}\right|_R = 0 \tag{5}$$

Using Eq.(2),(5) and the relation $\vec{v} = \vec{w} + \vec{\Omega} \times \vec{r}$ Eq.(4) becomes,

$$\frac{p}{\rho} + \frac{1}{2}\vec{w} \bullet \vec{w} - \frac{1}{2}(\vec{\Omega} \times \vec{r}) \bullet (\vec{\Omega} \times \vec{r}) = c \qquad (6)$$

Since the blades are identical and the 'free impeller' case is assumed, it suffices to consider a single blade channel.

2.2 Boundary layer dissipation loss

The dissipation loss in attached boundary layers can be quantified using a method based on a dissipation coefficient c_D (Schlichting [5]).
The dissipation power loss over a surface A of a rotating passage can be written as

$$\Delta P = \frac{1}{2}\rho \int c_D w^3 dA \qquad (7)$$

The estimate for c_D is 0.0038 for turbulent boundary layers with Re_θ of order 1000 (Denton [6]) and it has been the adopted value throughout the optimization process.

2.3 Numerical approach

The Laplace equation is solved numerically by COMPASS, a three-dimensional multi-block finite-element method which has been developed at the University of Twente, The Netherlands (Kruyt [7]). This method incorporates the super-element approach where systems of equations are solved by a direct method. By employing linear elements in combination with surface patch recovery (SPR) technique for velocity, second order accuracy for potential, velocity and pressure are obtained.

3 Optimization Method

3.1 Objective function

The weighted sum strategy converts the multi-objective problem of minimizing the vector F(x) into a scalar problem by constructing a weighted sum of all the objectives.

$$\min F(x) = \sum_{i=1}^{m} w_i \frac{f_i(x)}{f_i^{ref}} \qquad (8)$$

The weighting coefficients correspond to the relative importance of the objectives and allow tradeoffs between them to be expressed. The objective value $f_i(x)$ is divided by a reference value f_i^{ref} so that all terms have a similar order of magnitude.
The choice of the weighting coefficients associated with each objective changes the outcome of the optimization process and is thus an important task for the designer .
In this work, only hard constraints are considered and are prescribed as bounded domains. This means that upper and lower limits are imposed on all geometric parameters,

$$x_j \in [x_{j,\min}, x_{j,\max}] \qquad j=1\ldots N_{par} \qquad (9)$$

where N_{par} is the total number of parameters.

3.2 Blade Geometry Definition

The method proposed by van Os [1] is employed where the blade geometry is defined by a number of camber lines. The meridional projections of these camber lines are called construction lines, see Fig.[1]. On each of these construction lines the coordinates in the meridional plane (r, z) are given, together with a blade angle β that determines the amount of turning experienced by the fluid.

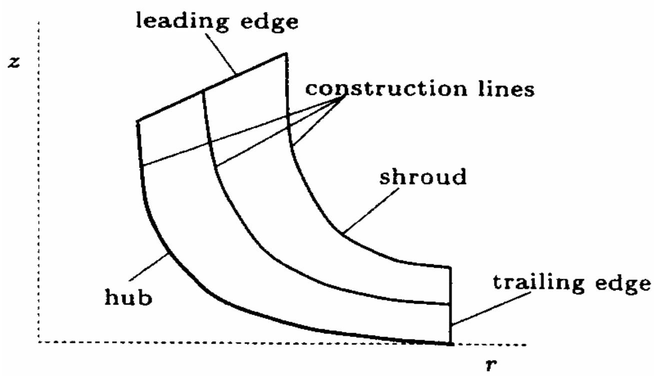

Fig.[1] Construction lines in the meridional plane.

The blade angle β is the angle between the camber line and the circumferential direction θ. The general blade angle definition reads,

$$\tan\beta = \frac{-dX_m}{rd\theta} \qquad (10)$$

The wrap angle θ can now be readily calculated by integrating Eq.[10] and using an offset for the trailing edge as a boundary condition.
By means of a cubic spline surface through the camber lines the final camber surface is constructed.
The thickness distribution is defined perpendicular and symmetrically to the camber surface to construct the blade surface.
By prescribing the meridional view and the blade angle distribution, a complete description of the blade in a cylindrical coordinate system (r,θ,z) is defined.

3.3 Hybrid Optimization Approach

After a certain number of iterations the exploration of the design space by the GA is assumed to have returned a solution in the close neighbourhood of the optimum where no local optima exist. The Pattern Search (PS) algorithm takes over from that point allowing further deterministic exploitation and faster convergence to be achieved. The scheme of the hybrid approach is depicted in Fig.[2].

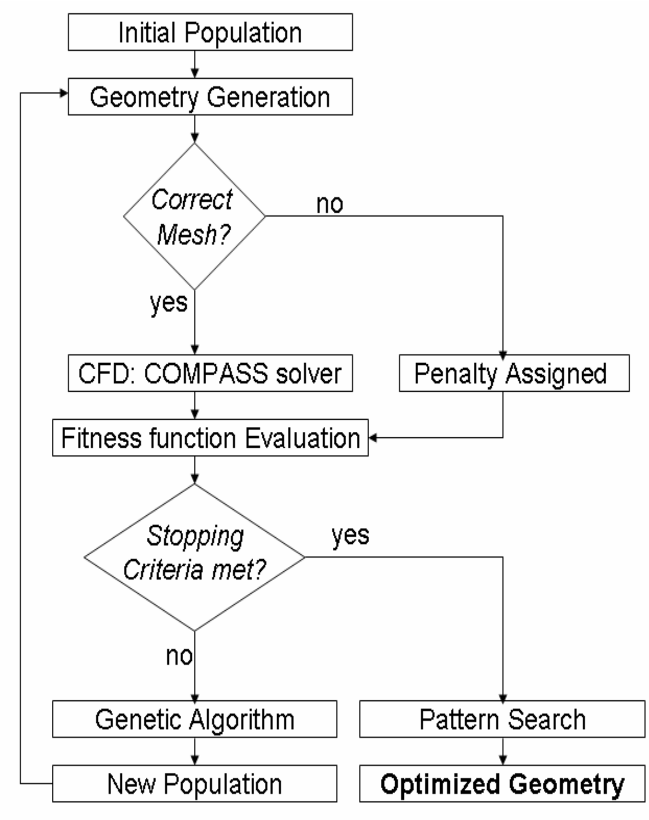

Fig.[2] Schematic of the optimization process.

Genetic Algorithm

GA's are a class of optimization methods based on the theory of natural evolution (Holland [8]). The main concept is that of "survival of the fittest" where a population of individuals (candidate geometries) evolves over the generations to reproduce better performing genes (geometry characteristics) while 'bad' traits of the population progressively die off.
The evolution process starts from a uniformly random population that obeys the restrictions imposed by Eq.[9]. The genetic algorithm uses this population to create the children that make up the next generation by applying 3 processes, (a) elitism (b) crossover and (c) mutation.
During elitism the individuals with the lowest fitness are automatically promoted to the next generation to preserve the best performing solutions. During the selection stage of crossover reproduction, two parent individuals are chosen from the population based on their fitness. The method here used is the roulette wheel selection: an individual has a probability k of being selected, where k is equal to the proportion of its fitness to the sum of all the fitness of the individuals in the current population. Then the crossover child is created by combining the vector entries of a pair of selected parents.
The mutation process involves randomly changing genes in the parent's vector entries. This operator reduces the probability of the algorithm to get stuck in local minima.
Table [1] summarizes the settings that have been used for the GA.

Population Size	150
Initial Population	uniform random
Generations	8
Elite members count	2
*Crossover fraction	80%
*Mutation Fraction	20%
Crossover selection	roulette wheel

*other than elite members

Table[1] Settings for the GA

Pattern Search

To explore the region around the GA's best solution we use a neighbourhood search strategy in which a direct search method is employed. A pattern is a collection of vectors that the pattern search algorithm uses to determine which points to search at each iteration. The basic idea is to establish a successful pattern of coordinate moves, and then to reapply this pattern exhaustively in the successful directions until no further reduction in the fitness function can be obtained (Sherif et al. [3]). Successive iterations repeat this process after establishing a new pattern with an adapted exploratory mesh size.
The pattern search starts with a base point, i.e. the solution returned from the genetic optimization. The directions in which the algorithm will search are the standard pattern vectors for the global pattern search 2 node positive basis. A move to a new point is established by multiplying the pattern vectors with a scaled mesh size and adding the resulting vectors to the base point. The algorithm then polls the mesh points by computing their objective function until a value is found that is lower than the fitness of the base point.
After a successful poll, the algorithm replaces the base point with the fitter one and expands the current mesh size by a factor of 2. If exploration

around the base point fails the algorithm does not change the base point at the next iteration but contracts the mesh size by a factor of 0.5. The process is terminated after a prescribed number of objective function evaluations.

4 Problem Definition

Among the main objectives of impeller design is the increase of total pressure of the fluid across the machine, called the head H of the pump. Furthermore, to avoid local reduction of the static pressure p to the vapour pressure p_v of the liquid (cavitation) the pressure drop on the blades should not exceed a design value (NPSH). Certain duty of the pump dictates the steepness of its characteristic Q-H curve along the working envelope while the power losses that occur within the impeller are to be minimized.

4.1 Objective function

The multi-point optimization was based on 2 working points, at the original design best efficiency point (BEP) and at an increased flow rate by 15.7% of BEP. The second point was used to evaluate the steepness of the Q-H characteristic.

The following objectives have been imposed,

- Maximum Head
- Minimum $NPSH_i$
- Maximum efficiency η
- Maximum steepness $d\Psi/d\Phi$

The estimate on the NPSH inception value has been based on the minimum pressure along the vanes starting from 3% blade length. The incipient NPSH is defined by

$$NPSH_i = \frac{p_0^i - p_v}{\rho g} \qquad (11)$$

where p_0^i is the stagnation pressure at the inlet corresponding to the beginning of cavitation and p_v is the vapour pressure of the fluid.

The four objectives together with their corresponding weighting coefficients are used to construct the scalar fitness function. The weighting has been tuned so that the objectives of head, efficiency and steepness were treated with the same level of importance. The objective of $NPSH_i$ was given a relative lower weight contributing less to the absolute value of the fitness function.

4.2 Geometry Parametrization

If all the possible geometrical parameters of an impeller were set as optimization variables, this would result in a far too large design space for an efficient optimization to take place.

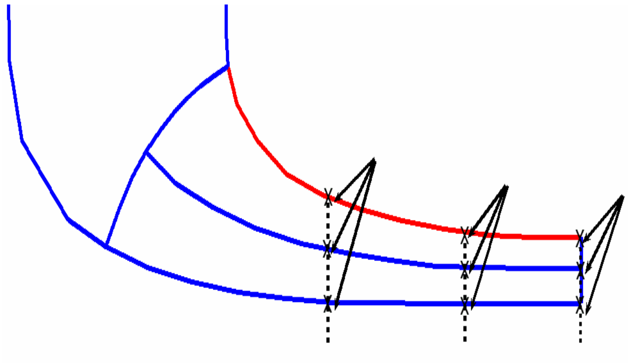

Fig.[3] Position of parametric blade angles.

A thorough investigation by experienced designers has led to the key-choice of the interesting geometrical degrees of freedom.

The meridional profile is defined by 3 construction lines at hub, mid-span and shroud of the blade. The blade angle distribution is determined by 3 beta values along each construction line at 2 fixed radii and at the trailing edge, see Fig.[3]. A cubic spline interpolation is used to evaluate all the intermediate points. The blade angles at exactly the leading edge were fixed from experience.

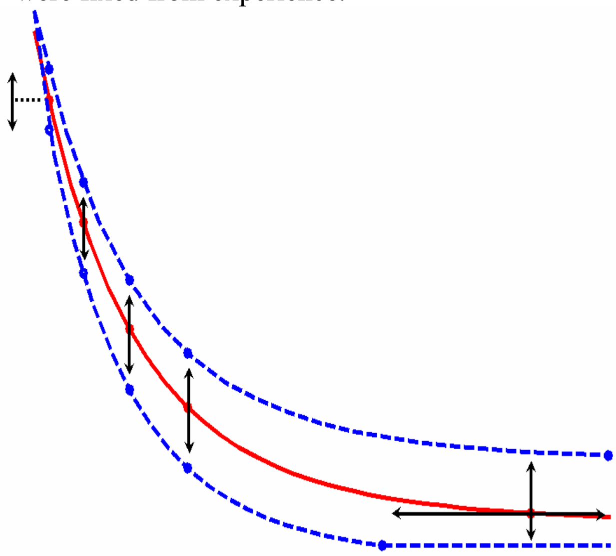

Fig.[4] Shroud curve, degrees of freedom for the 5 construction points.

The shroud curve is defined by 5 construction points. The 4 points closest to the leading edge were left to vary in the axial direction within certain bounds, see Fig.[4]. The point closest to the trailing edge received an extra degree of freedom in the radial direction that determined the starting of a purely radial part (lowest construction line in Fig.[4]). The axial value of the latter point directly controls the outlet width of the impeller. To assure

the smoothness of the shroud curve a power series interpolation was used to refine the position of the 5 construction points and to determine all the intermediate ones. Construction lines at hub and mid-span were unchanged.
The thickness distribution superimposed on the blade surface along with the actual number of blades was kept constant as in the original design. The described geometry parameterization results in a total number of 15 variables.

5 Results

The convergence history of the optimization process can be seen in Fig.[5].

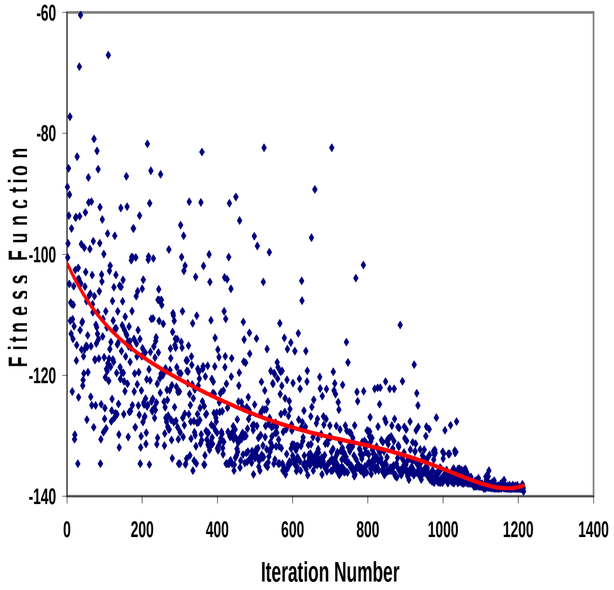

Fig.[5] Convergence history

The first and largest part of the history corresponds to the exploration of the search space by the GA. During this stochastic part of the optimization a great dispersion of fitness values can be observed which slowly converge to a mean value. A more organized pattern and a faster convergence is apparent from iteration 1050, when pattern search is initiated. This is caused by the deterministic, local character of the method. The zero-gradient of the mean fitness value near the end of the optimization indicates that pattern search has exhausted the search in the close neighborhood of GA's best individual. For a number of candidate geometries a valid mesh could not be generated. These geometries have been penalized and excluded from the convergence history. The depicted number of iterations in Fig.[5] has been reduced to 1220 from a total of 1400.
The results of the optimization are summarised in Table[2]. All objectives are presented for the original and the optimized impeller design along with their percentage of variation.

		Original	Optimized	Change %
Head	(Ψ)	0.534	0.606	+13.3
Efficiency	(η)	96.34	97.27	+0.96
$NPSH_i$	(κ)	0.179	0.172	-3.91
Steepness	($d\Psi/d\Phi$)	4.677	3.789	+18.9
Fitness value		-112.54	-136.34	-21.1

Table [2] Comparison of performance objectives

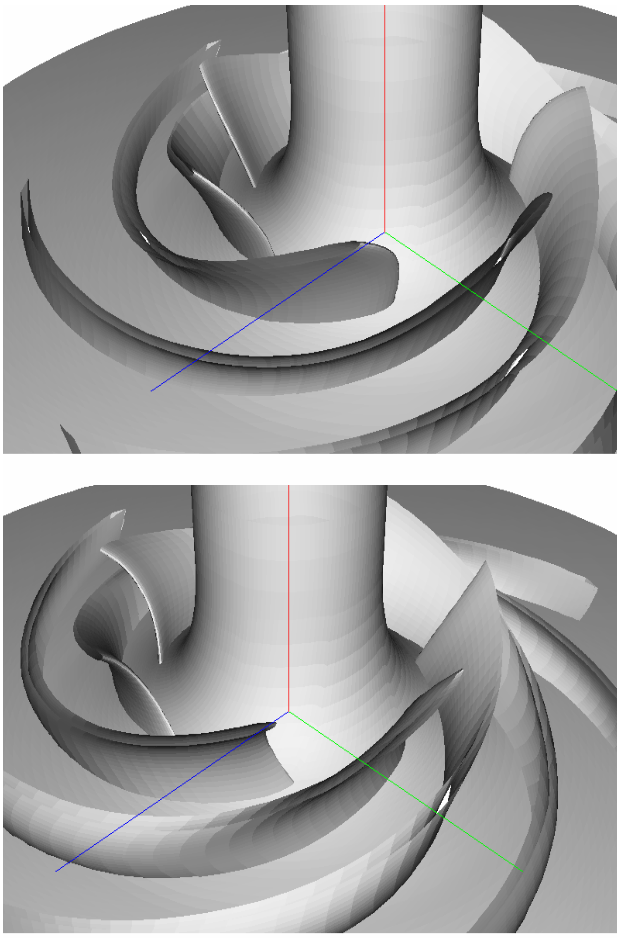

Fig.[6] 3D view of original and optimized (lowermost) design.

The improvement in the $NPSH_i$ value, a reduction of 3.91%, can be attributed to the change of the blade angle after the leading edge. The change in shape of the leading edge can be clearly seen in Fig.[7] where original and optimized blades are overlapping.

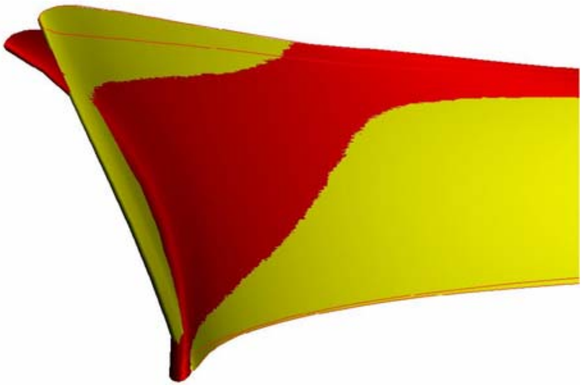

(a)

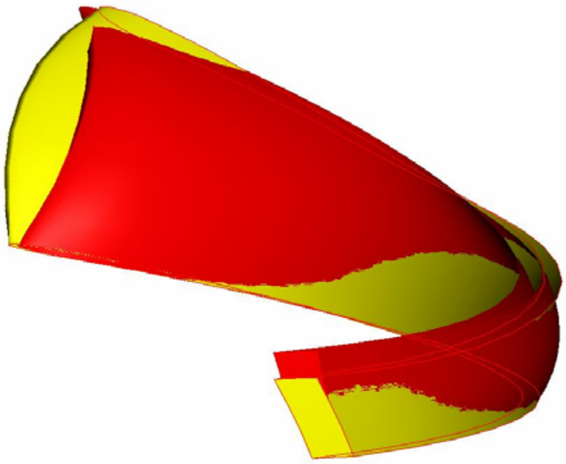

(b)

Fig.[7] Geometry differences at (a) Leading Edge and (b) across the blade. Note the change in width at the trailing edge.

The geometry of the optimized design has a higher outlet width than the original design, see Fig.[8]. This leads to lower relative velocities in the impeller channel which in turn result, for the same blade angles, to higher efficiency and higher head.

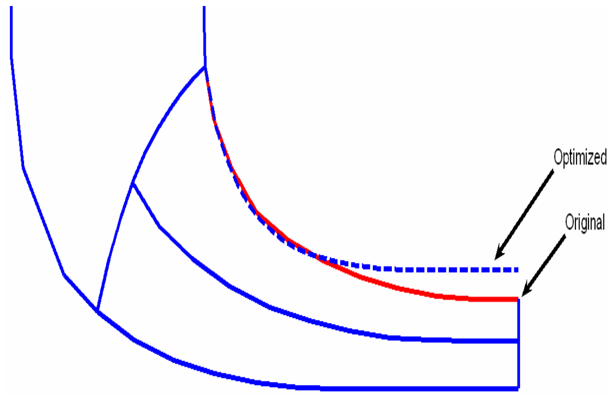

Fig.[8] Meridional view for optimized and original design

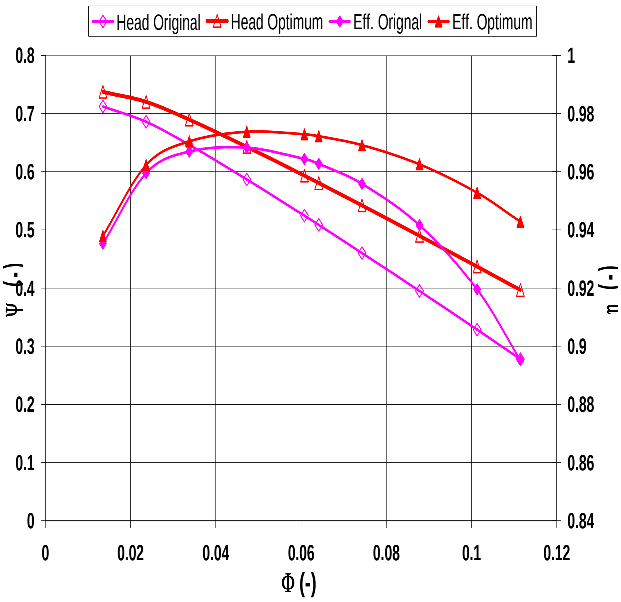

Fig.[9] Head and Efficiency characteristics of original and optimized design.

Performance characteristics are presented in Fig.[9] and Fig.[10]. A major increase in head and efficiency is achieved for the optimized design, see Fig.[9]. A significant reduction in NPSH requirements is also achieved as in Fig.[10]. Over a large range of working flow rates the optimized design is superior to the original.

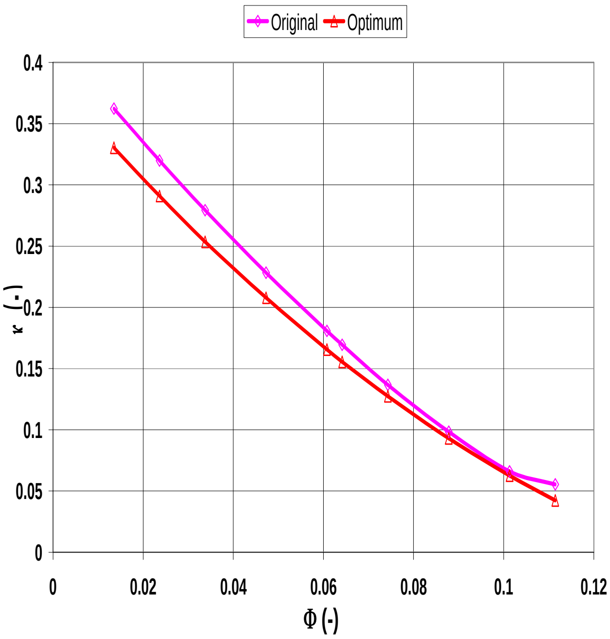

Fig.[10] NPSH characteristics with respect to 3% blade length of original and optimized design.

In Fig.[11], [12], [13] the objectives of head, efficiency and steepness versus each other are presented. The latter objectives are scattered for all the evaluated geometries.

In Fig.[12] it is shown that an increase of head results to an increase in efficiency. A higher head is caused by higher blade angles at the trailing edge. This in turn results in shorter blades and a decreased surface for viscous phenomena to occur. Furthermore, an increase in impeller width which would give a higher head by reducing the relative velocities also diminishes power losses which are proportional to the relative velocities, see Eq.[7].

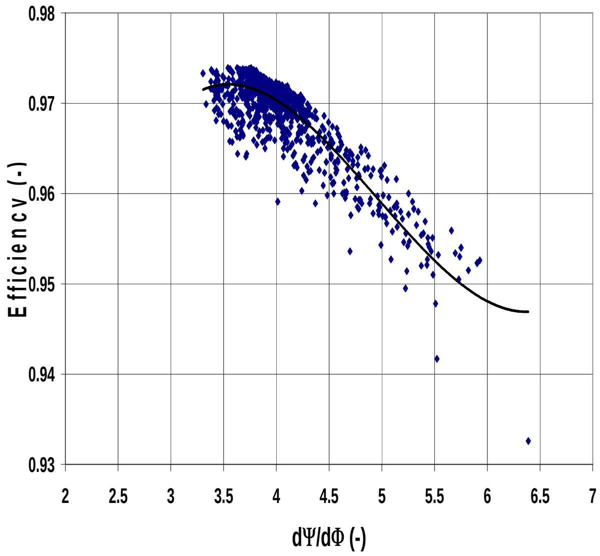

Fig.[11] Efficiency related to steepness of Q-H curve.

Fig.[11] and Fig.[13] show the contradictory goals that are captured in the fitness function. A high steepness value of dΨ/dΦ, a steeper curve in Fig.[9], limits the head factor and hydraulic efficiency that can be achieved. This is expected, as from a simple velocity triangle approach which shows higher steepness and lower heads with decreasing outlet blade angle values.

It has been demonstrated that efficiency and head are complementary performance objectives. On the contrary steepness is contradictory to both head and efficiency. From Table [2] it can be concluded that head, efficiency and $NPSH_i$ have been improved whereas the objective of steepness has deteriorated. The selection of weighting coefficients determines the tradeoff between such contradictory objectives and the final quality of the optimized design.

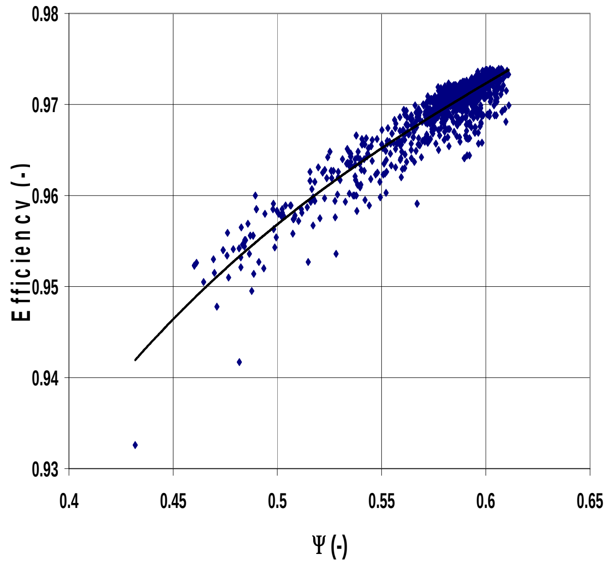

Fig.[12] Efficiency related to the head factor.

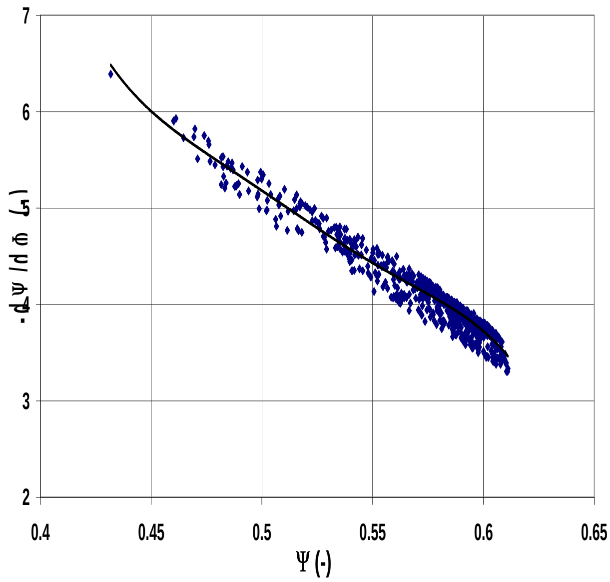

Fig.[13] Steepness of Q-H curve related to the head factor.

6 Conclusions

The performance of an industrial radial-flow pump impeller has been optimized. A potential flow model has been employed to simulate the flow inside the blade channel. Performance characteristics are calculated at each iteration to compute the single scalar value of the multi-objective cost function. The designer has to choose and weight the objectives to be included in the cost function, an assignment which pilots the optimization process and essentially affects the final solution.

The method shows a global optimum in a design space of 15 geometrical parameters. The current design example showed an improvement for head, efficiency and $NPSH_i$ which clearly demonstrates the power of the method used. These performance characteristics have been improved at a minimum expense of the contradictory objective of steepness. Timescales needed to setup the problem and computational requirements are reasonable to make the application of the method feasible for industrial use.

Acknowledgements

The authors wish to thank the management of Flowserve for their support and permission to publish this paper. Our colleagues/mentors J.G.H. Op de Woerd, B.J. Boersma and N.P. Kruyt are thanked for providing valuable advice throughout this study.

References:

[1] van Os, Marijn J., 1998, “On the flow and cavitation inception of mixed-flow impellers” , Ph.D. dissertation, Department of Mechanical Engineering, University of Twente, Enschede, Netherlands

[2] Van Esch, B. P. M., Kruyt, N. P., 2001, Hydraulic performance of a mixed-flow pump: Unsteady inviscid computations and loss models, Journal of Fluids Engineering, Vol 123, pp. 256-264

[3] Sherif, Y.S., Boice, B.A., Optimization by pattern search, European Journal of Operational Research 78 (1994) 277-303 , North-Holland

[4] Esch, B. P. M. van, 1997, ”Simulation of three-dimensional unsteady flow in hydraulic pumps”, Ph.D. dissertation, Department of Mechanical Engineering, University of Twente, Enschede, Netherlands

[5] Schlichting, H., Boundary Layer Theory, McGraw-Hill,NY,1979

[6] Denton, J.D., 1993, “Loss mechanisms in Turbomachines”, ASME J. Turbomach., 115, pp. 621-656

[7] Kruyt, N. P.,2003 Compass 4.00 user manual. University of Twente.

[8] Holland JH. Adaptation in natural and artificial systems. Ann Arbor: University of Michigan Press; 1975.

[9] Kelder, J. H. D., Dijkers, R. J. H., van Esch, B. P. M., and Kruyt, N. P., 2001 “Experimental and theoretical study of a low specific speed pump”. Fluid Dynamics Research, 28(4), pp. 267-280

[10] Goldberg, D.E., “Genetic Algorithm”, Addison Wesley, 1994

[11] Dijkers, R. J. H., Visser, F. C., and Op de Woerd, J. G. H., 2000, Redesign of high-energy centrifugal pump first stage impeller, *I. A. H. R.*, Charlotte, North Carolina, U.S.A.

[12] Van Esch, B. P. M., Kruyt, N. P. and Jonker, J. B., 1997, An inviscid-viscous coupling method for computing unsteady flows entire pump configurations. FEDSM97-3373. In Proceedings of the 1997 ASME Fluids Engineering Division Summer Meeting, Vancouver, Canada.

[13] Van Os, M.J., Op de Woerd, J.G.H. and Jonker, J.B., 1997, A parametric study of the cavitation inception behaviour of a mixed-flow pump impeller using a three-dimensional potential-flow model. FEDSM97-3374. In Proceedings of the 1997 ASME Fluids Engineering Division Summer Meeting, Vancouver, Canada.